Mikrostrukturbasierte Materialmodellierung diskontinuierlich faserverstärkter Verbundwerkstoffe

T. Böhlke, B. Brylka, V. Müller

Institute of Engineering Mechanics, Karlsruhe Institute of Technology (KIT)

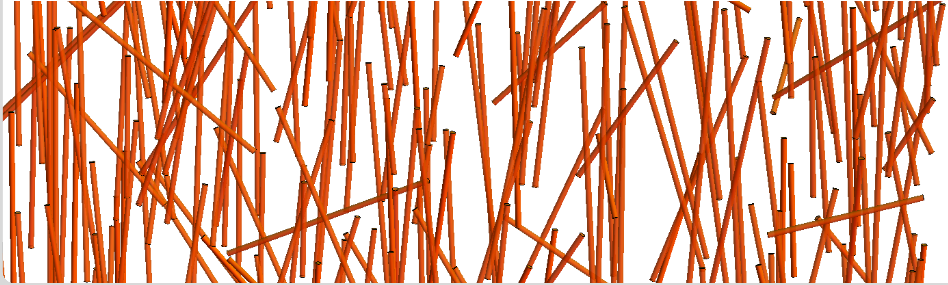

Outline

Application and Properties of Composites

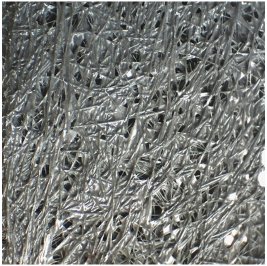

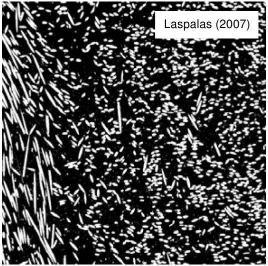

Laspalas (2007)

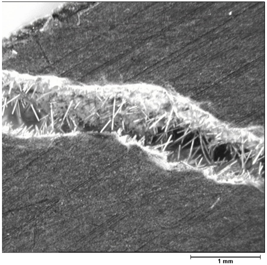

thecarbonfiberjournal.com

press photo BASF

hilti.de

Outline

InnoSMC: Investigation of Effective Stiffness of Sheet-Moulding-Compounds (SMC)

Karlsruhe Institute of Technology

Mould filling simulation

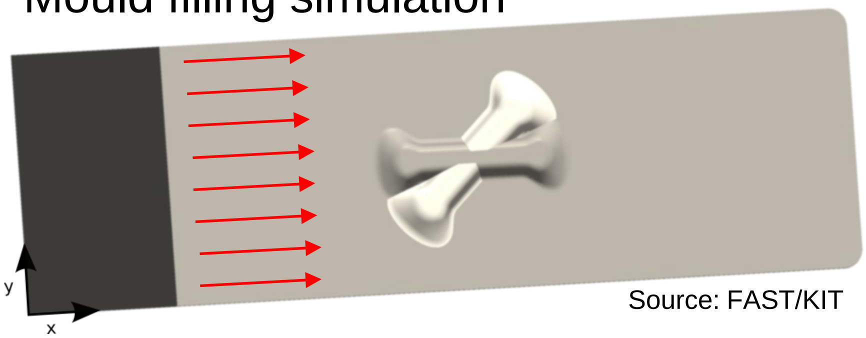

Source: FAST/KIT

Local material orientation

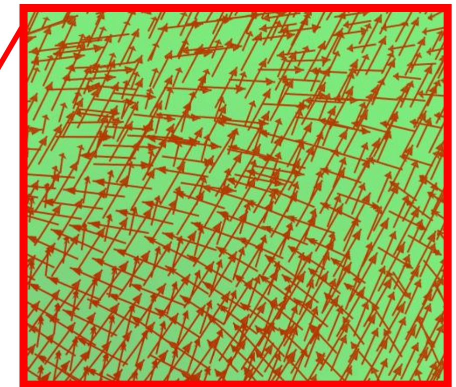

FE-simulation

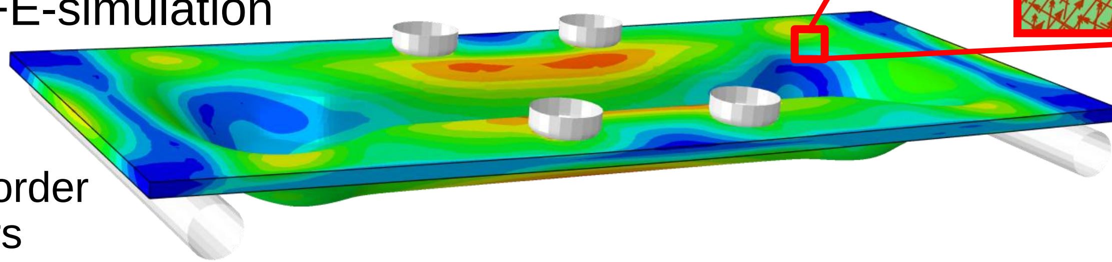

- Mapping of 2nd order orientation tensors
- Closure approximation of 4th order orientation tensors
- Homogenization of local stiffness tensors

Experiment

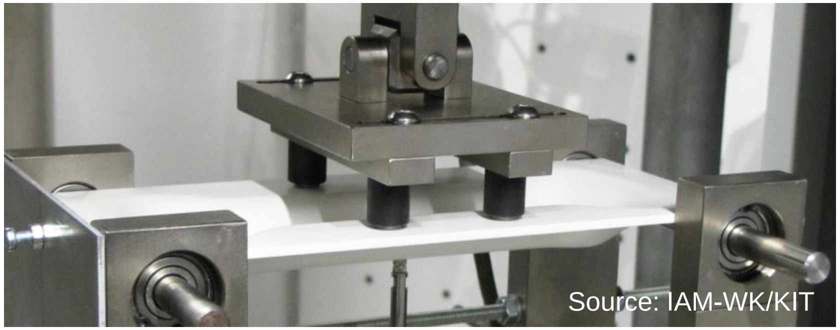

Europäische Union
Europäischer Fonds für regionale Entwicklung

investition in Ihre Zukunft!

Baden-Württemberg

InnoSMC: Investigation of Effective Stiffness of Sheet-Moulding-Compounds (SMC)

Karlsruhe Institute of Technology

Results of
mould filling simulation

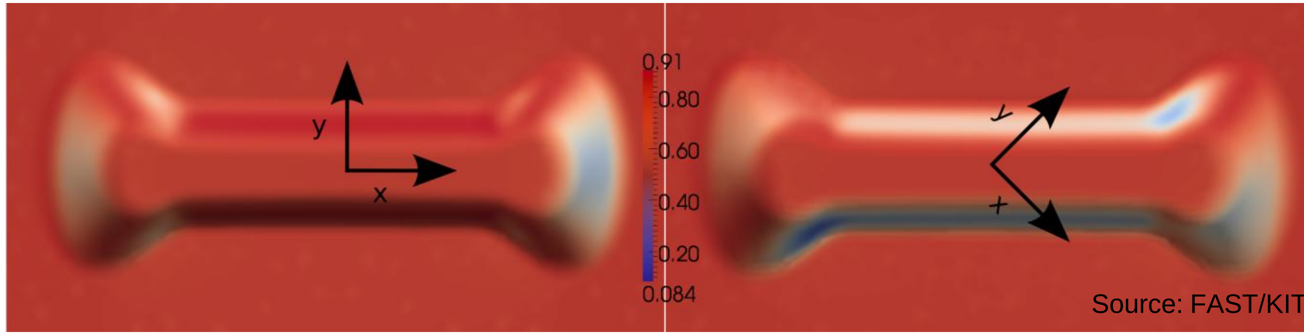

Results of
FE-simulation

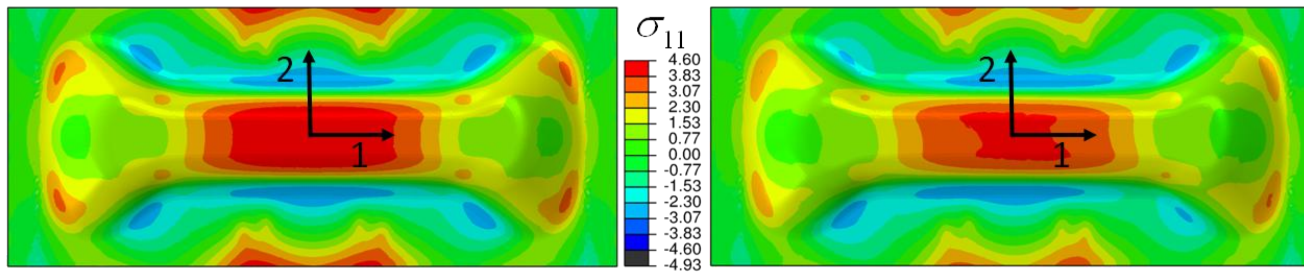

Comparison of
simulation and
experiment

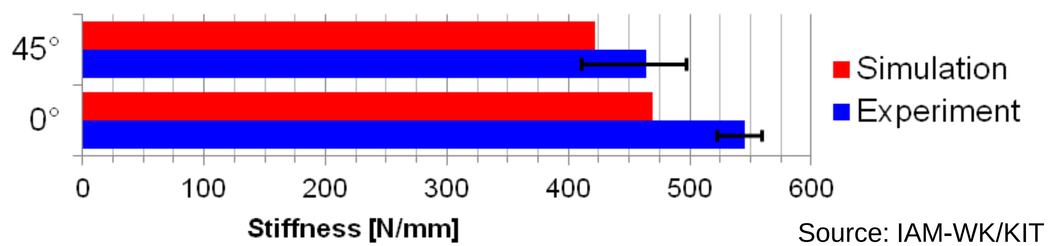

Source: IAM-WK/KIT

Europäische Union
Europäischer Fonds für regionale Entwicklung

investition in
Ihre Zukunft!

Baden-Württemberg

Die gezeigten Ergebnisse resultieren aus dem Forschungsprojekt InnoSMC (www.fast.kit.edu/lbt/InnoSMC.php). Das Vorhaben wird durch die Europäische Union - Europäischer Fonds für regionale Entwicklung - sowie das Land Baden-Württemberg gefördert. Die Verwaltungsbehörde des operationellen Programms RWB-EFRE ist das Ministerium für Ländlichen Raum, Ernährung und Verbraucherschutz Baden-Württemberg. Weitere Informationen stehen unter www.rwb-efre.baden-wuerttemberg.de zur Verfügung.

Outline

1 Motivation

2 Modelling of the SMC process chain

3 Scale bridging based on tomography data

4 How to describe the orientation distribution of fibers?

5 Experimental identification of constitutive behaviour

6 Conclusions

Objective

target part

- manufacturing process
- material properties
- fraction of reinforcements
- geometry of reinforcements

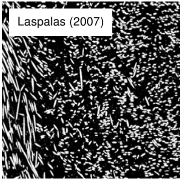

material analysis

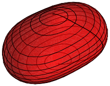

effective Young's modulus

- aspect ratio
- orientation
- fraction

microstructure parameter

METHOD
BOX

Method 1: 2-Step-Approach

e.g. Advani et al. (1987), Willis (1977)

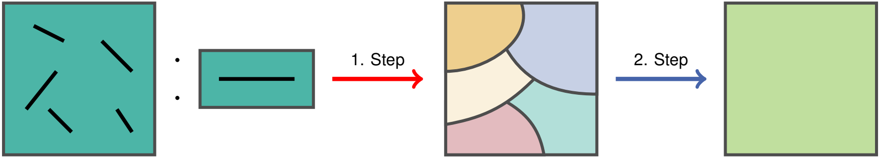

1. Step:

$$\mathbb{C} = \{\mathbb{C}_{\mathsf{M}}, \mathbb{C}_{\mathsf{I}}\} \qquad c = \{c_{\mathsf{M}}, c_{\mathsf{I}}\} \qquad \mathbb{P}_0 = \mathbb{P}_0(\mathbb{C}_0, \boldsymbol{A})$$

$$\bar{\mathbb{C}}_{\mathsf{UD}} = \sum_{\alpha=1}^{2} c_\alpha \mathbb{C}_\alpha \left[\mathbb{I}^{\mathsf{s}} + \mathbb{P}_0(\mathbb{C}_\alpha - \mathbb{C}_0)\right]^{-1} \left\{ \sum_{\beta=1}^{2} c_\beta \left[\mathbb{I}^{\mathsf{s}} + \mathbb{P}_0(\mathbb{C}_\beta - \mathbb{C}_0)\right]^{-1} \right\}^{-1}$$

lower bound

$$\bar{\mathbb{C}}_{\mathsf{UD}}^{\mathsf{HS}^-} \to \mathbb{C}_0 = \mathbb{C}_{\mathsf{M}}$$

upper bound

$$\bar{\mathbb{C}}_{\mathsf{UD}}^{\mathsf{HS}^+} \to \mathbb{C}_0 = \mathbb{C}_{\mathsf{I}}$$

Method 1: 2-Step-Approach

e.g. Advani et al. (1987), Willis (1977)

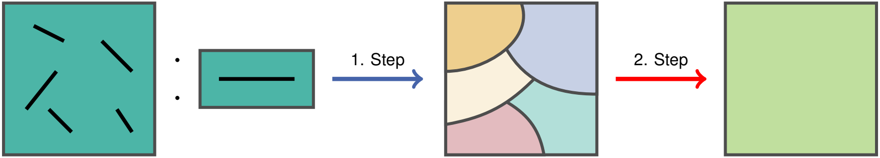

2.A. Step: Simple Bounds

$$\bar{\mathbb{C}}^V = \sum_{\alpha=1}^{n} c_\alpha \mathbb{C}_\alpha \qquad \bar{\mathbb{S}}^R = \sum_{\alpha=1}^{n} c_\alpha \mathbb{S}_\alpha$$

2.B. Step: Second Order Bounds ($\mathbb{C} = \bar{\mathbb{C}}^\alpha_{\mathsf{UD}}$, $c = c^\alpha$, $\mathbb{P}_0 = \mathbb{P}_0(\mathbb{C}_0, \boldsymbol{A}^\circ)$)

$$\bar{\mathbb{C}} = \sum_{\alpha=1}^{n} c_\alpha \mathbb{C}_\alpha \left[\mathbb{I}^{\mathsf{s}} + \mathbb{P}_0(\mathbb{C}_\alpha - \mathbb{C}_0)\right]^{-1} \left\{ \sum_{\beta=1}^{n} c_\beta \left[\mathbb{I}^{\mathsf{s}} + \mathbb{P}_0(\mathbb{C}_\beta - \mathbb{C}_0)\right]^{-1} \right\}^{-1}$$

lower bound

$$\bar{\mathbb{C}}^{\mathsf{HS}^{--}} \rightarrow \mathbb{C}_0 = \min\big(\mathrm{iso}\,(\bar{\mathbb{C}}_{\mathsf{UD}})\big)$$

upper bound

$$\bar{\mathbb{C}}^{\mathsf{HS}^{++}} \rightarrow \mathbb{C}_0 = \max\big(\mathrm{iso}\,(\bar{\mathbb{C}}_{\mathsf{UD}})\big)$$

Method 2: Self-Consistent Scheme

e.g. Willis (1981)

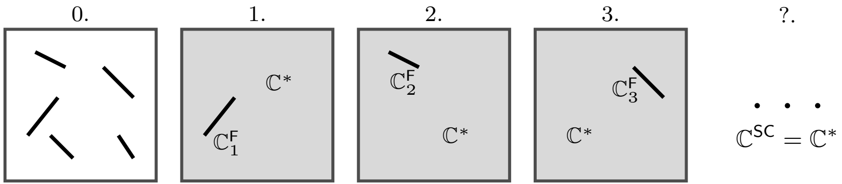

Effective elastic stiffness and strain localization

$$\mathbb{C}^{\mathsf{SC}} = \mathbb{C}_{\mathsf{M}} + \sum_{\alpha=1}^{N} c_\alpha \left(\mathbb{C}_\alpha - \mathbb{C}_{\mathsf{M}}\right) \mathbb{A}_\alpha^{\mathsf{SC}} \qquad \mathbb{A}_\alpha^{\mathsf{SC}} = \left(\mathbb{I}^{\mathsf{s}} + \mathbb{P}_0^{\mathsf{SC}} \left(\mathbb{C}_\alpha - \mathbb{C}^{\mathsf{SC}}\right)\right)^{-1}$$

Self-Consistent polarization tensor

$$\mathbb{P}_0^{\mathsf{SC}}(\mathbb{C}^{\mathsf{SC}}, \boldsymbol{A}) = \frac{1}{4\pi\sqrt{\det(\boldsymbol{A})}} \int_{\|\boldsymbol{n}\|=1} \mathbb{H}(\boldsymbol{n}) \frac{1}{\left(\boldsymbol{n} \cdot \boldsymbol{A}^{-1}\boldsymbol{n}\right)^{3/2}} \, \mathrm{d}n$$

with

$$\mathbb{H}(\boldsymbol{n}) = \mathbb{I}^{\mathsf{s}}(\boldsymbol{K}^{-1} \square (\boldsymbol{n} \otimes \boldsymbol{n}))\mathbb{I}^{\mathsf{s}} \qquad K_{ij} = C_{irjs}^{\mathsf{SC}} n_r n_s$$

Example: Short Fiber Reinforced PP (PPGF30)

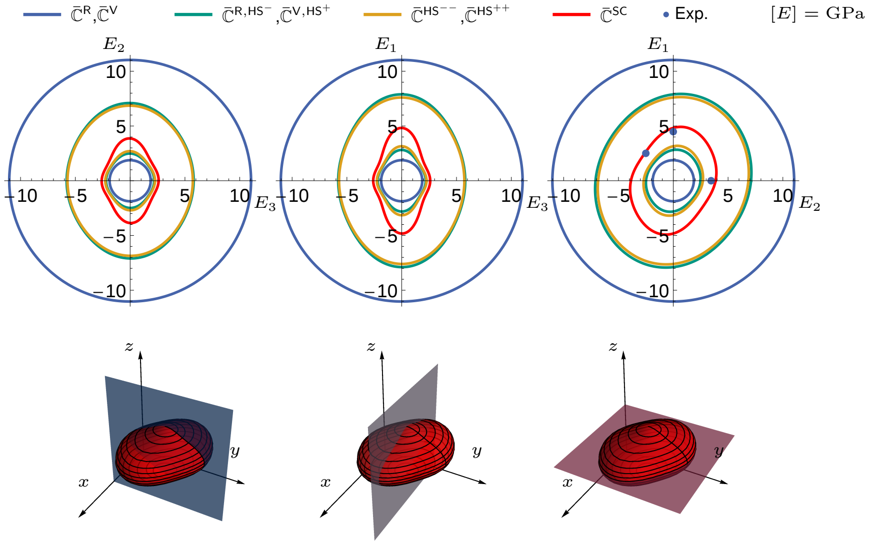

Virtual Tensile Test a)

max. principle stress on real microstructure

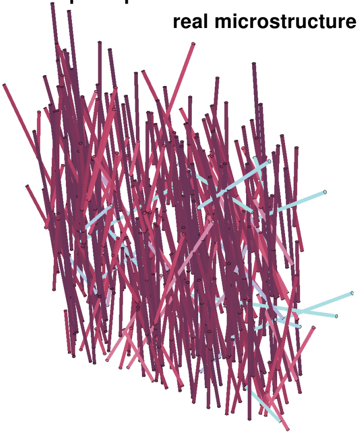

pole figure of the principle stress

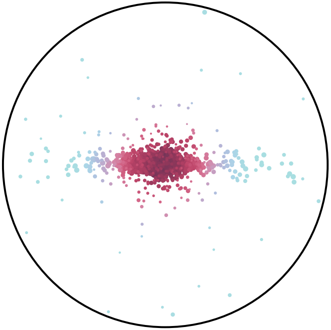

stress histogram

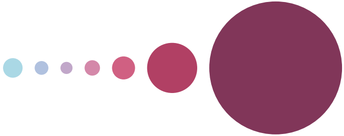

legend

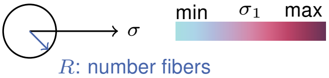

Virtual Tensile Test b)

max. principle stress on real microstructure

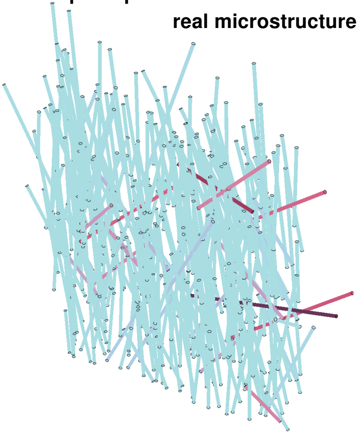

pole figure of the principle stress

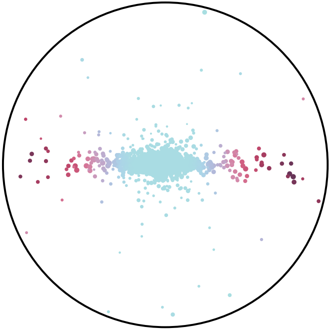

stress histogram

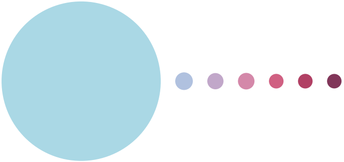

legend

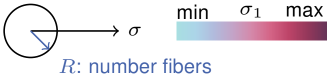

Outline

Fiber Orientation Distribution Function (FODF)

Folgar (1983), Advani et al. (1987), Böhlke (2010)

Fiber orientation

$$\boldsymbol{c} = \sin(\vartheta)\sin(\varphi)\boldsymbol{e}_1 + \sin(\vartheta)\cos(\varphi)\boldsymbol{e}_2 + \cos(\vartheta)\boldsymbol{e}_3$$

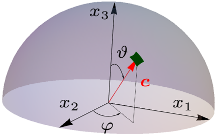

v.Mises-Fisher distribution

$$\frac{\mathrm{d}v}{v}(\boldsymbol{c}) = f_c(\boldsymbol{c})\,\mathrm{d}c \qquad f_c(\boldsymbol{c}) = \frac{\kappa}{\sinh(\kappa)}\exp(\kappa\,\bar{\boldsymbol{c}}\cdot\boldsymbol{c})$$

$\bar{\boldsymbol{c}}$: reference axis

κ: concentration

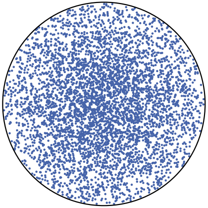

$\kappa = 0.01$

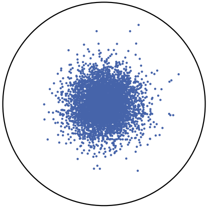

$\kappa = 10$

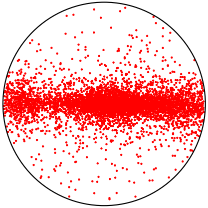

real μct data

Maximum Entropy Principle

Jaynes (1957), Jaynes (1957), Wu (1997), Böhlke (2005), Junk et al. (2012)

Expansion of FODF

$$f_c(\boldsymbol{c}) = 1 + \boldsymbol{D}_2' \cdot (\boldsymbol{c} \otimes \boldsymbol{c})' + \mathbb{D}_4' \cdot (\boldsymbol{c} \otimes \boldsymbol{c} \otimes \boldsymbol{c} \otimes \boldsymbol{c})' + \dots \qquad (\cdot)'\text{: irreducible part}$$

Problem

given: leading moment tensors $\boldsymbol{D}_2', \dots$

wanted: statistical consistent estimate of the distribution density $f_c(\boldsymbol{c})$

Conditions

nonnegative: $f_c(\boldsymbol{c}) \geq 0 \quad \forall\, \boldsymbol{c}$

normalized: $\int_{\|\boldsymbol{c}\|} f_c(\boldsymbol{c})\, \mathrm{d}c = 1$

Note, that a truncation of the series after n items violates the consistency conditions:

$$\bar{f}_c(\boldsymbol{c}) = 1 + \sum_{i=1}^{n} \mathbb{D}_{2i}' \cdot \left(\boldsymbol{c}^{2i\otimes}\right)' \ngeq 0 \qquad \left(\boldsymbol{c}^{2i\otimes}\right) = \underbrace{\boldsymbol{c} \otimes \boldsymbol{c} \otimes \cdots}_{2i-\text{times}}$$

Entropy Maximization for Axis Symmetric Microstructures

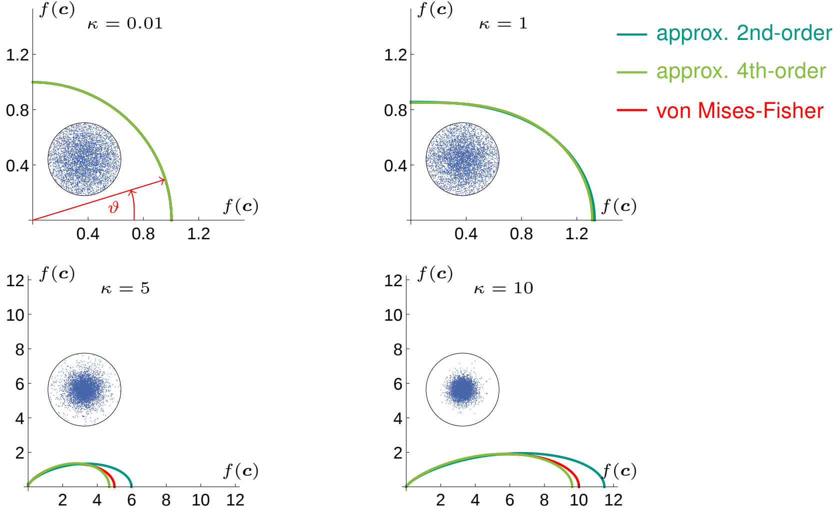

Outline

Material Behaviour of LFT Manufactured in Compression Moulding Process

- Anisotropic material stiffness and strength
- Non-linear stress-strain relation

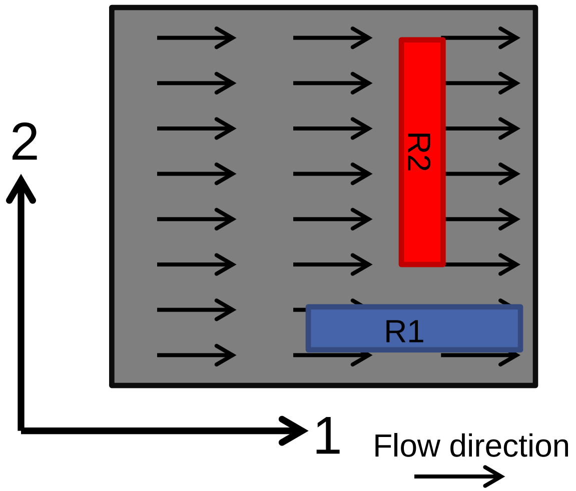

Quasi-static tension

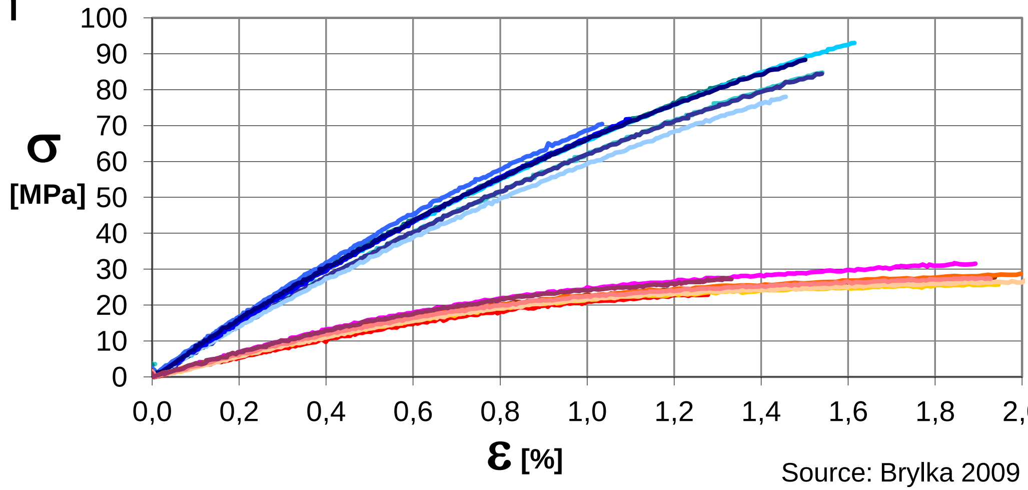

Source: Brylka 2009

- Anisotropic damage initiation and evolution
- Temperature and strain-rate sensitivity

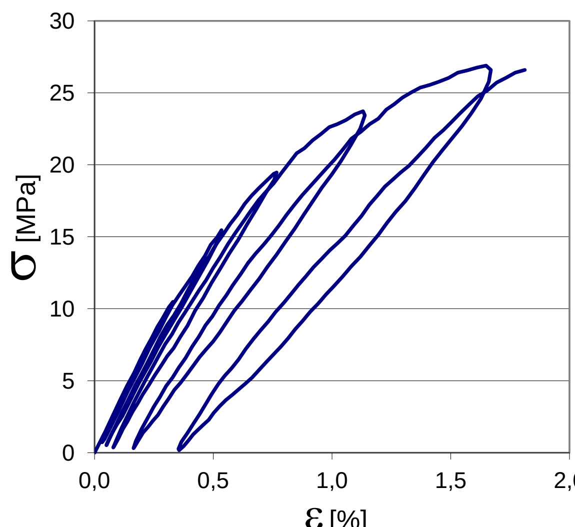

Source: Brylka 2009

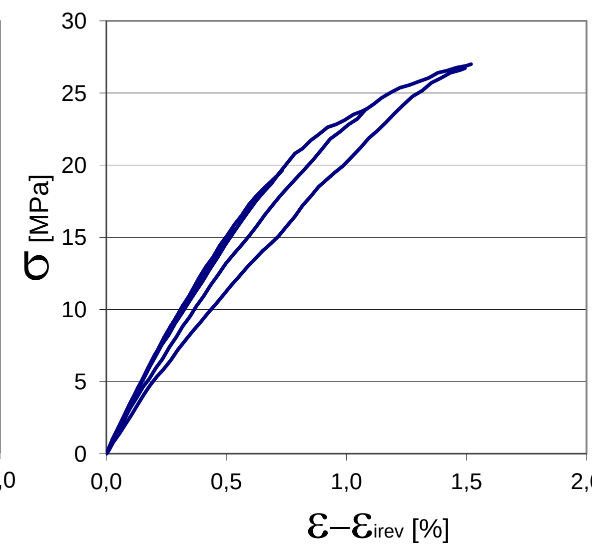

Material system: PPGF30
Matrix: Polypropylen
Fibres: glass fibres, 20mm initial length

Experimental Results for Polypropylene Matrix: Storage Modulus in Temperature Frequency Sweeps

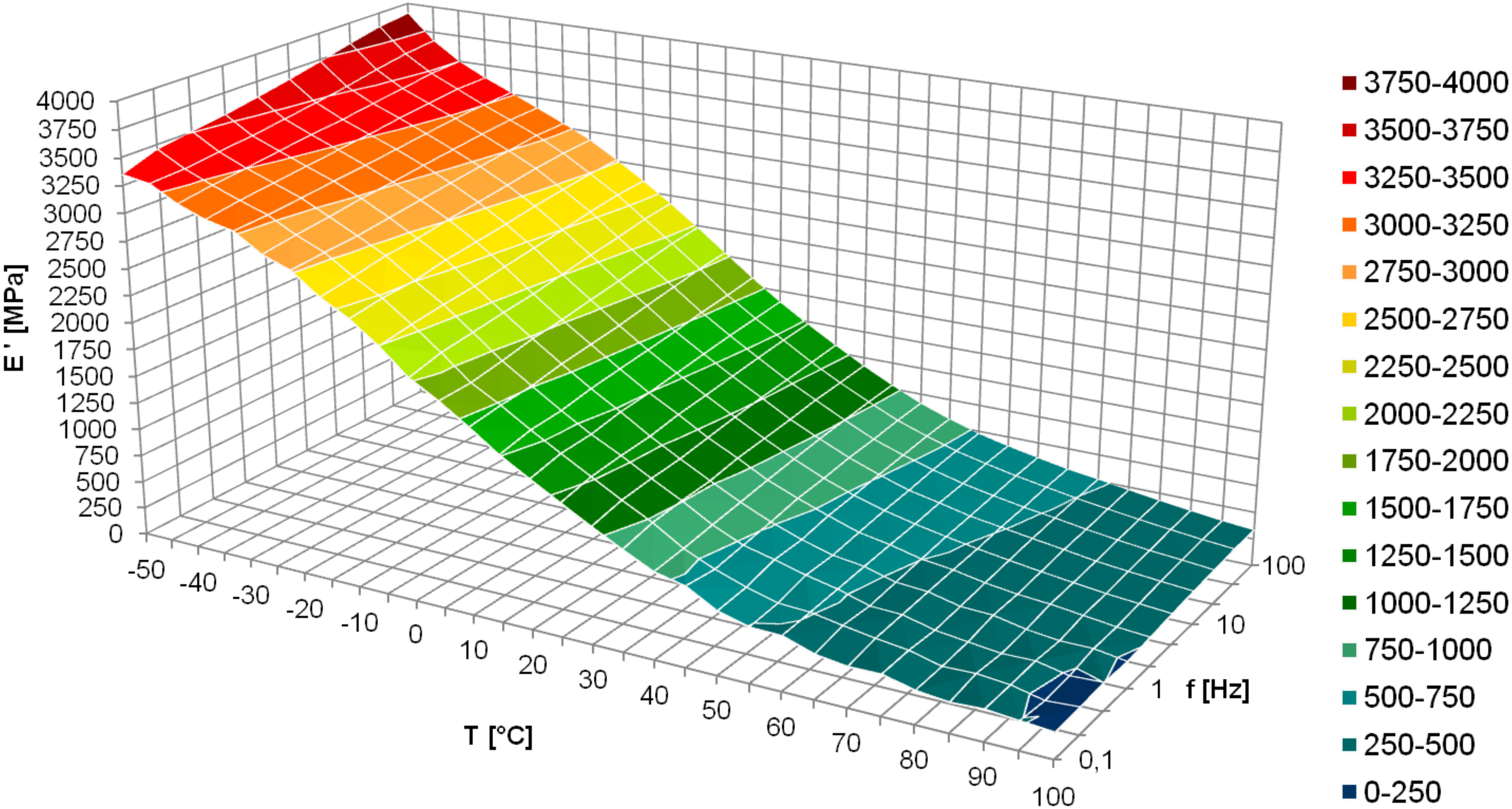

Constant parameters: $\overline{\sigma}_0 = 5MPa, \quad \tilde{\varepsilon}_0 = 0{,}025\,\%$

Experimental Results for Polypropylen Matrix: Loss Modulus in Temperature Freqeuncy Sweep

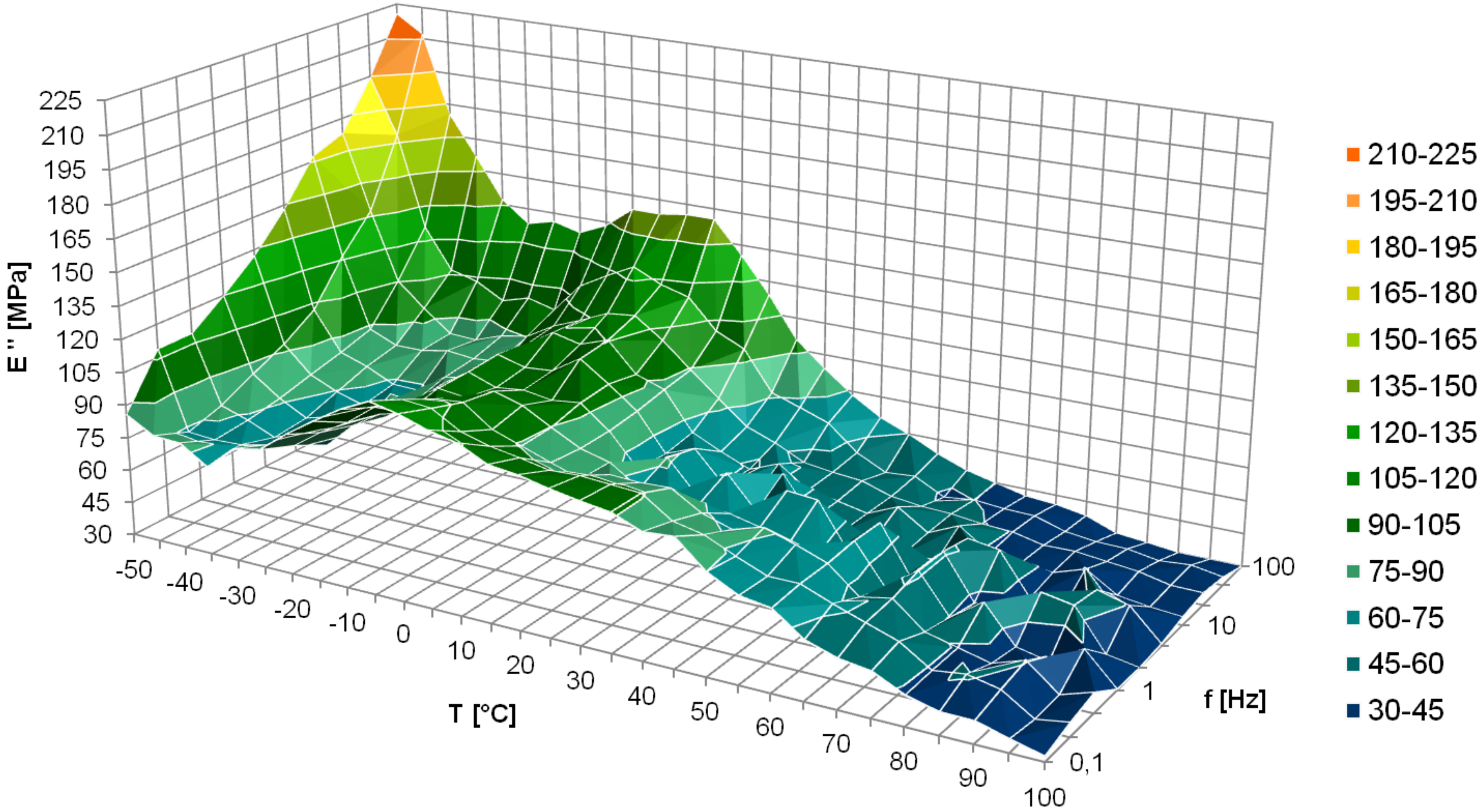

Constant parameters: $\bar{\sigma}_0 = 5MPa, \quad \tilde{\varepsilon}_0 = 0{,}025\,\%$

Experimental Results of DMA Measurments: Comparison of PP and LFT

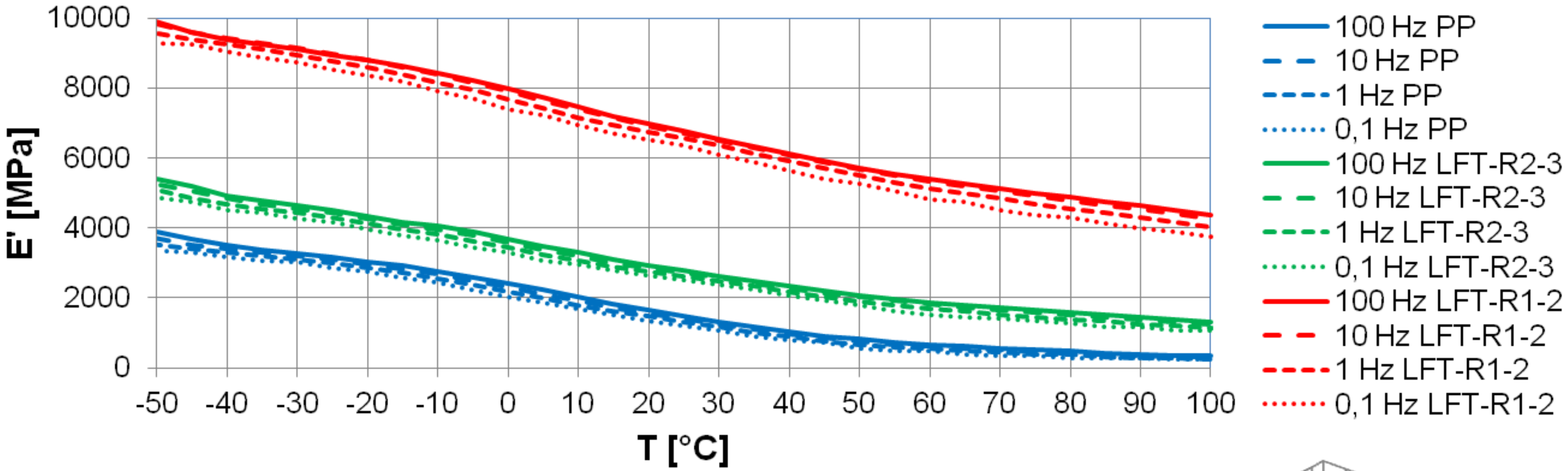

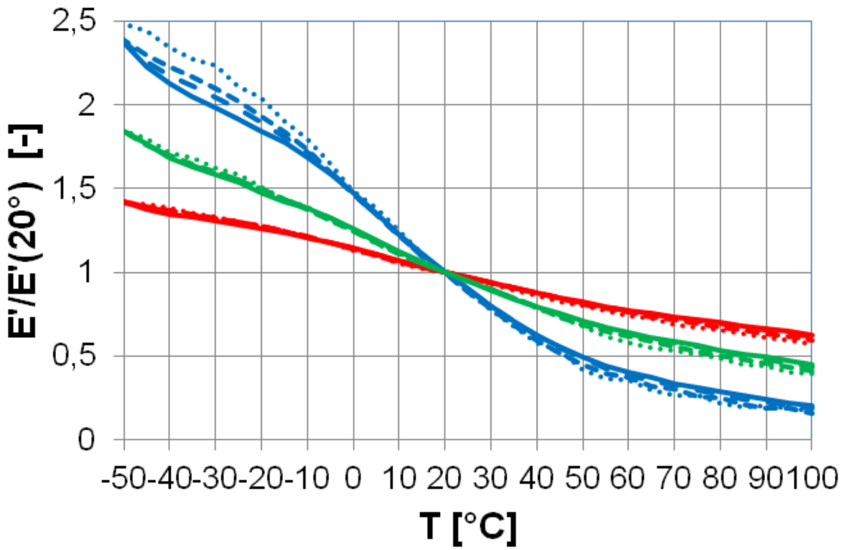

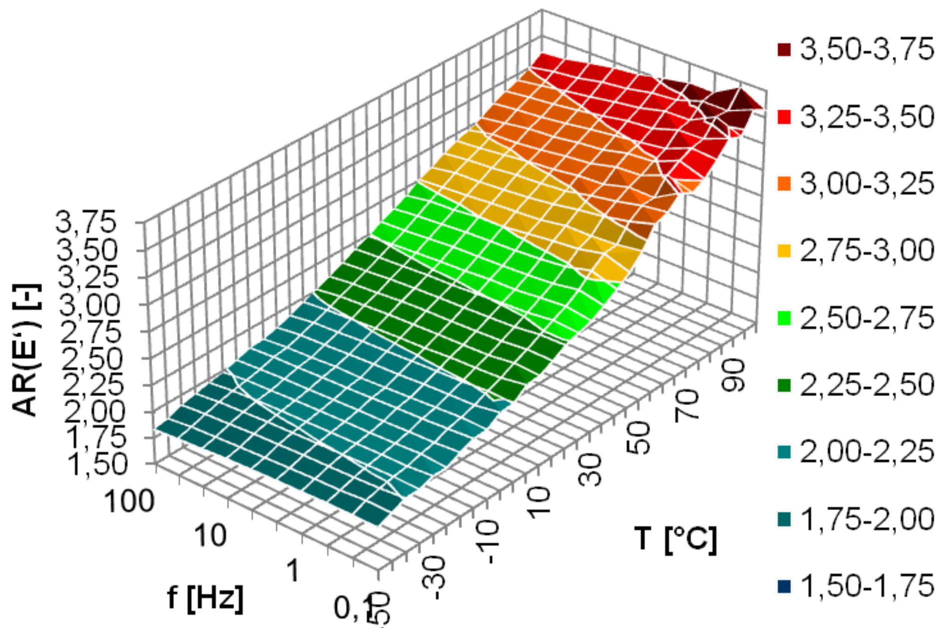

Frequency Dependent Damage of LFT

1. Time-Sweep
Dynamic measurement
Static stress= 2 MPa
Stress amplitude=1,5 MPa
Frequnecy= 10 Hz
Time= 2500 s

2. Frequency-Sweep
Dynamic measurement
Static stress= 2 MPa
Stress amplitude=1,5 MPa
Frequnecy= 0,5-50 Hz

3. Tension test
Quasistatic measurement
Strain rate= 10^-4 1/s
Maximum stress= (2,5 MPa)* n

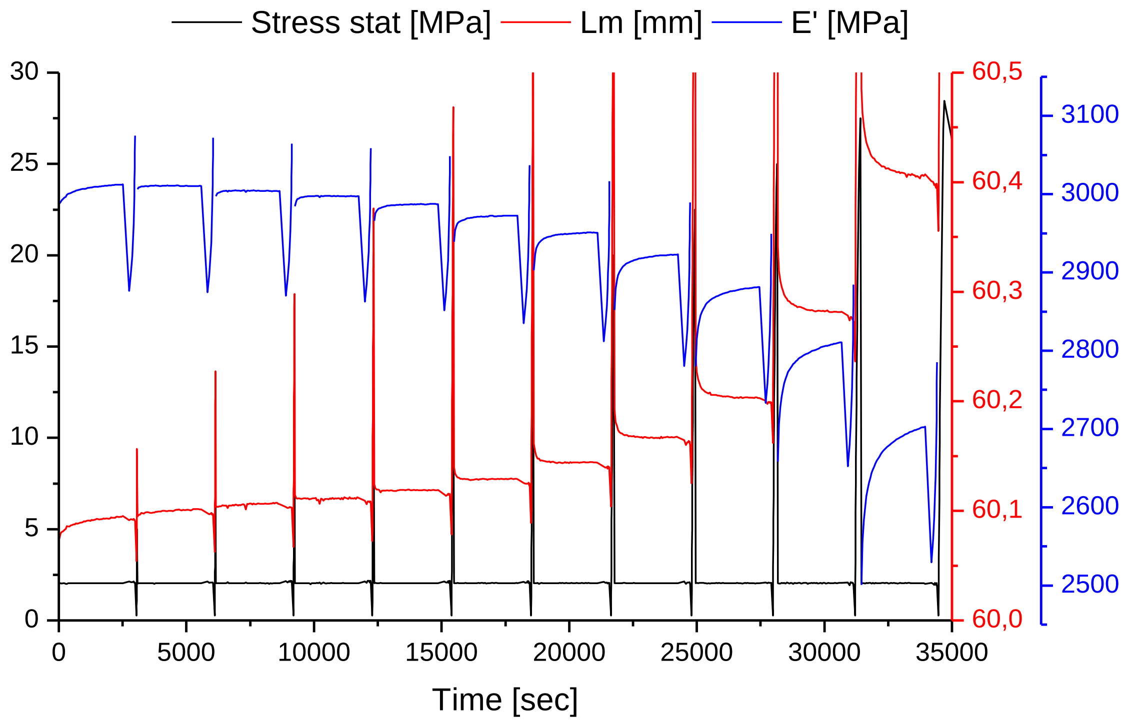

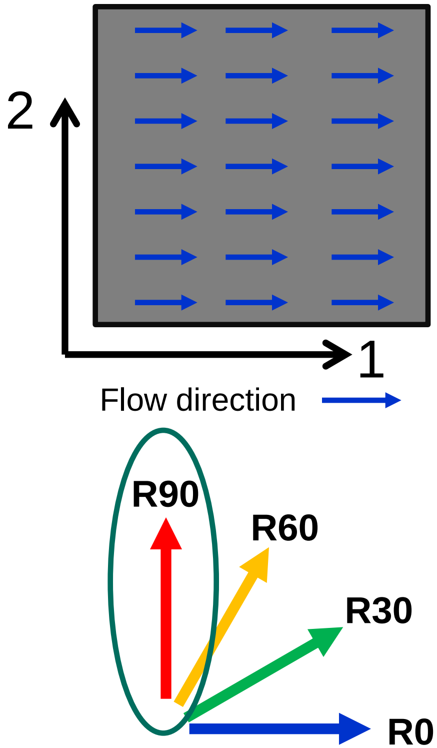

Experimental DMA Results of Stiffness Degradation

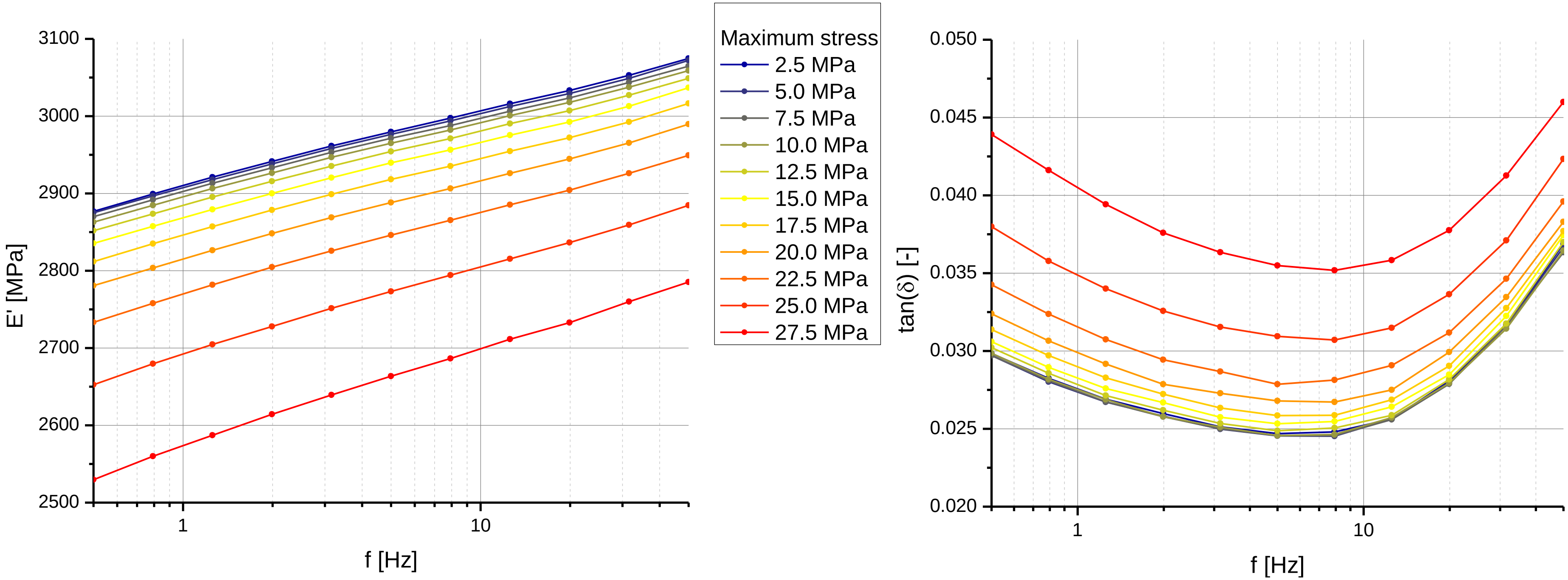

Measurement at 20°C in the R90 direction of the composite

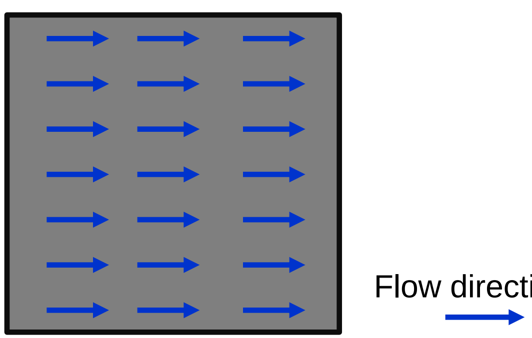

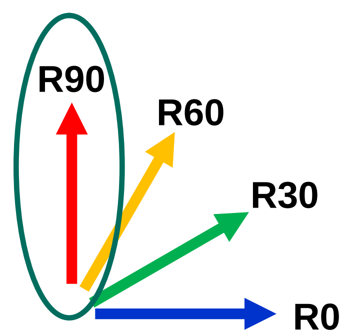

Stiffness Degradation of LFT

Definition of frequency dependent damage: $D(f,\sigma_{max}) = 1 - \dfrac{E'(f,\sigma_{max})}{E'(f,\sigma_{max}=\sigma_0)}$

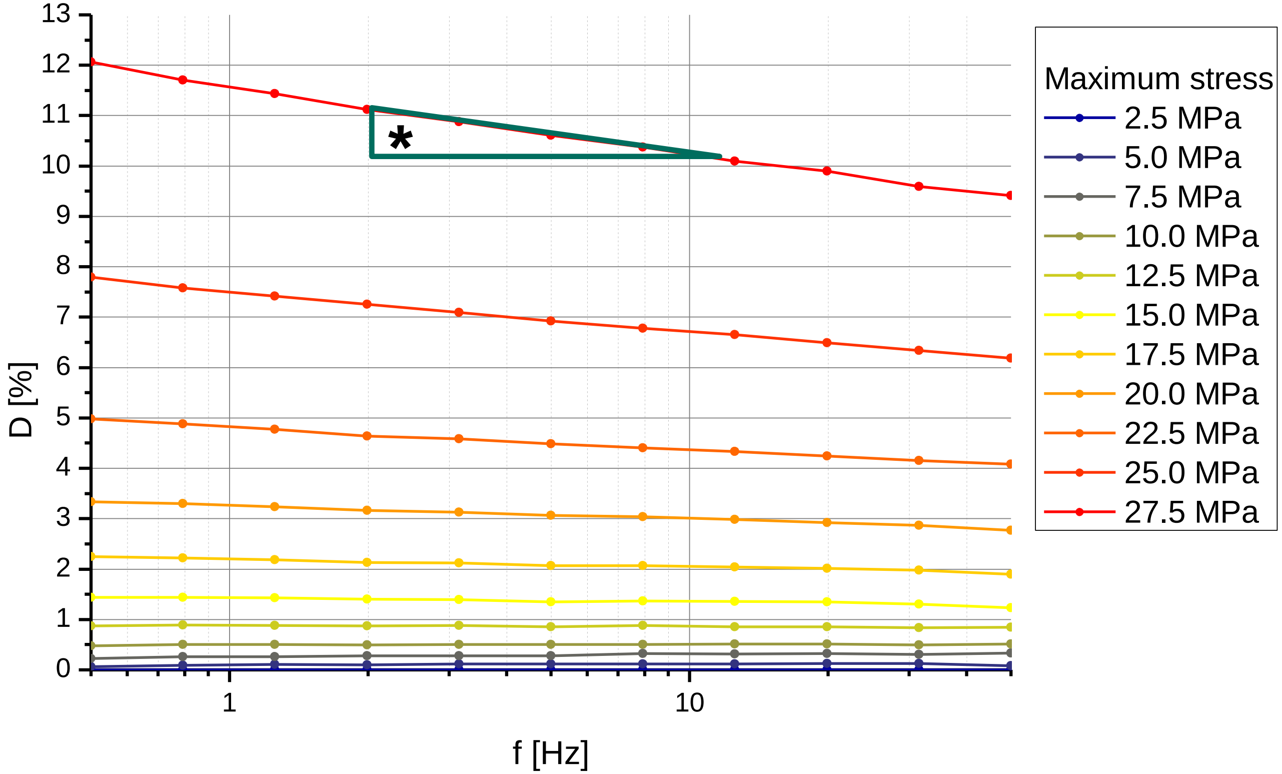

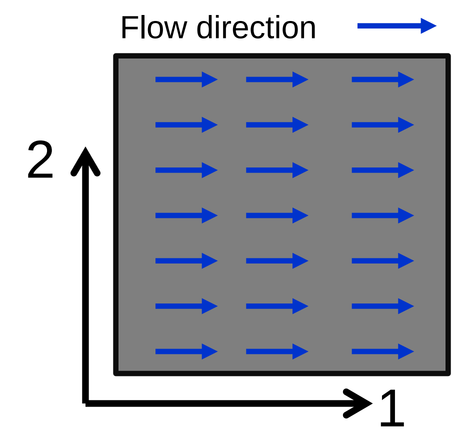

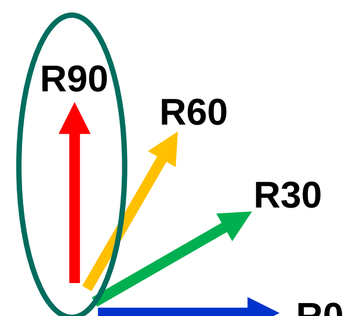

Damage evolution at 20°C by loading in R90 direction

* $dD/df \quad [\%/\log(Hz)]$

Outline

Conclusions

Karlsruhe Institute of Technology

- Process simulation takes into account lower-order orientation information. For low degrees of texture anisotropy the coupling of fluid and solid type simulations based on second-order orientation tensors is a robust model approach.
- Higher-order moments of the fiber orientation distribution function can be estimated based on the maximum entropy principle (MEP). MEP gives statistically consistent estimates of the orientation distribution function based on statistically incomplete information.
- The classical self-consistent scheme evaluated with tomography data gives accurate estimates of the effective elastic properties. The self-consistent scheme will be extended in order to include thermally induced eigenstrains.
- The anisotropy and stiffness of LFT are strongly temperature and frequency dependent.
- The stiffness degradation and its rate depends on frequency, temperature and loading direction.

Acknowledgement

Partners in InnoSMC at KIT

- FAST: Sven Sanwald, Frank Henning
- IAM-WK: Benjamin Bertram, Kay André Weidenmann

Die gezeigten Ergebnisse resultieren aus dem Forschungsprojekt InnoSMC (www.fast.kit.edu/lbt/InnoSMC.php). Das Vorhaben wird durch die Europäische Union - Europäischer Fonds für regionale Entwicklung - sowie das Land Baden-Württemberg gefördert.

Europäische Union
Europäischer Fonds für regionale Entwicklung

investition in Ihre Zukunft!

Baden-Württemberg

Die Verwaltungsbehörde des operationellen Programms RWB-EFRE ist das Ministerium für Ländlichen Raum, Ernährung und Verbraucherschutz Baden-Württemberg. Weitere Informationen stehen unter www.rwb-efre.baden-wuerttemberg.de zur Verfügung.

Partners at Fraunhofer LBF

- Felix Dillenberger, Robert Glöckner

Partner at Giessen University of Applied Sciences

- Stefan Kolling